Arabian Journal of Chemistry (2022) **15**, 103687

King Saud University

Arabian Journal of Chemistry

www.ksu.edu.sa
www.sciencedirect.com

ORIGINAL ARTICLE

C-methyl flavonoid from the leaves of *Cleistocalyx conspersipunctatus*: α-glucosidase inhibitory, molecular docking simulation and biosynthetic pathway

Haifang Du [a,b,c], Hanxiang Li [b], Ping Wu [b,c,*], Jinghua Xue [b], Yunshan Wu [a,d], Xiaoyi Wei [b,c], Bo Liu [a,d,e,*]

[a] *Guangdong Provincial Key Laboratory of Clinical Research on Traditional Chinese Medicine Syndrome, The Second Clinical Medical College, Guangzhou University of Chinese Medicine, Guangzhou 510006, PR China*
[b] *Key Laboratory of Plant Resources Conservation and Sustainable Utilization, South China Botanical Garden, Chinese Academy of Sciences, Xingke Road 723, Tianhe District, Guangzhou 510650, PR China*
[c] *University of Chinese Academy of Sciences, Yuquanlu 19A, Beijing 100049, PR China*
[d] *Guangzhou Key Laboratory of Chirality Research on Active Components of Traditional Chinese Medicine, Guangzhou 510006, PR China*
[e] *State Key Laboratory of Dampness Syndrome of Chinese Medicine, Guangzhou 510120, PR China*

Received 6 October 2021; accepted 4 January 2022
Available online 10 January 2022

KEYWORDS

Cleistocalyx conspersipunctatus;
C-methyl flavonoids;
α-Glucosidase inhibition;
Molecular docking;
Biosynthetic pathway

Abstract We extracted one new *C*-methyl flavonoid, farrerol 7-*O*-*β*-D-(6-*O*-galloyl) glucopyranoside (**1**), along with 11 known flavonoids, from the *Cleistocalyx* (*C.*) *conspersipunctatus* leaves. Elucidation of these flavonoid structures was accomplished through spectroscopic investigation and electronic circular dichroism (ECD) computation. Compared to corosolic acid (IC_{50}: 15.5 ± 0.9 μM), an established inhibitor, the compound **1** (IC_{50}: 6.9 ± 1.2 μM) was found more active in suppressing α-glucosidase. These findings imply the potential of compound **1** as a valid α-glucosidase inhibitor, which also offer evidence for future animal experiments and clinical trials. Besides, molecular docking was employed to explore the probable mechanism for α-glucosidase–

* Corresponding authors at: Key Laboratory of Plant Resources Conservation and Sustainable Utilization, South China Botanical Garden, Chinese Academy of Sciences, Xingke Road 723, Tianhe District, Guangzhou 510650, PR China (Ping Wu). Guangdong Provincial Key Laboratory of Clinical Research on Traditional Chinese Medicine Syndrome, The Second Clinical Medical College, Guangzhou University of Chinese Medicine, Guangzhou 510006, PR China (Bo Liu).
E-mail addresses: wuping@scbg.ac.cn (P. Wu), doctliu@263.net (B. Liu).
Peer review under responsibility of King Saud University.

Production and hosting by Elsevier

https://doi.org/10.1016/j.arabjc.2022.103687

compound **1** interaction. The biosynthetic pathway of these flavonoids in *C. conspersipunctatus* were proposed.

1. Introduction

Cleistocalyx conspersipunctatus Merr. et Perry (*C. conspersipunctatus*), an evergreen Myrtle tree indigenous to China's Hainan (Editorial Committee of Flora of China, 1984), is utilized as timber (xylem) by natives. *Cleistocalyx operculatus,* its closest relative, is extensively grown in China's southern regions (e.g. Guangdong, Hainan), as well as countries like Indochina Peninsula, India, Malaysia, Indonesia and Oceania. In Vietnam and China, there is a long history of *C. operculatus* medication (leaves and flower buds) for managing diverse conditions, such as antidiabetic activities (Editorial Committee of the Administration Bureau of Traditional Chinese Medicine, 1999). *C*-methyl flavonoids are a unique group of naturally occurring flavonoids. *C*-methyl on the flavonoid scaffold increases the cell membrane permeability of this class of compounds and subsequently benefits their bioactivity. We isolated 7 flavonoids from the leaves of *C. operculatus*, of which the 3′,5′-dimethylated chalcone 2′,4′-dihydroxy-6′-methoxy-3′,5′- dimethylchalcone (DMC) is important members of *C*- methyl flavonoids, which exhibit prominent anti-tumor activity (Zhu et al., 2005; Ye & Lai, 2016). Besides, five novel pentacyclic triterpenoids were lately isolated by us from the *C. conspersipunctatus* leaves, which exhibit α-glucosidase inhibitory activity (Du et al., 2021). For structural diversity expansion of the biofunctional *C*-methyl flavonoids and searching of more bioactive novel analogues, a further exploration was made by us on the *C. conspersipunctatus* leaves, eventually identifying a brand-new *C*-methyl flavonoids, 7-*O*-*β*-D-(6-*O*-galloyl) glucopyranoside (**1**), along with 11 known flavonoids (**2**–**12**) (Fig. 1). Among them, the new compound **1** exhibited potent α-glucosidase inhibitory activity. α-glucosidase (EC3.2.1.20) is an essential enzyme that hydrolyzes carbohydrates in catabolism to produce energy-metabolizing sugars (Chiba, 1997). In addition, it is well known that α-glucosidase is directly related to type II diabetes mellitus (DM). Due to the potential clinical application in treatment of type II DM, various studies on plant-derived α-glucosidase inhibitors have been reported (Fang et al., 2022; Ning et al., 2019). Therefore, researchers have potential influences on the research of α-glucosidase. Molecular docking was employed to explore the α-glucosidase–compound **1** interaction. The flavonoid biosynthetic pathway in *C. conspersipunctatus* was proposed. The mechanism of flavonoid biosynthesis in the leaves of *C. conspersipunctatus* is largely unknown. Therefore, a systematic analysis of the regulatory enzymes involved in the biosynthesis of flavonoids during the development of *C. conspersipunctatus* leaves will help to target and artificially regulate the biosynthesis of specific flavonoids. In this work, the extraction, bioactivity, structural elucidation, molecular docking and biosynthetic pathway of compound **1** were elaborated. The finding contributed to grasping the interactive mechanism between the flavonoid and α-glucosidase, and to designing a novel α-glucosidase inhibitor.

2. Materials and methods

2.1. General experimental procedures

A polarimeter (Perkin-Elmer 341; PerkinElmer, USA) was utilized for assessing the optical rotations, where the solvent was MeOH. CD data were recorded in MeOH using a Chirascan CD spectrometer (Applied Photophysics Ltd.,England) using 50 nm/min scanning speed, 1 nm bandwidth, and three accumulations. For documentation of NMR spectra (1D and 2D), an Avance III spectrometer (500 MHz) from Bruker was utilized. A maXis Q-TOF mass spectrometer from Bruker was adopted for collection of HRESIMS data, while an API2000 LC/MS/MS instrument (AB SCIEX, USA) was used for acquisition of ESIMS data. An HPLC system with a LC-6AD pump (Shimadzu, Japan) was utilized for preparative HPLC, where a 5 μm 10 × 250 mm column (YMC-pack ODS-A, YMC, Japan) was used at a 2 mL/min flow rate. Column chromatography (CC) was performed on 100–200 mesh

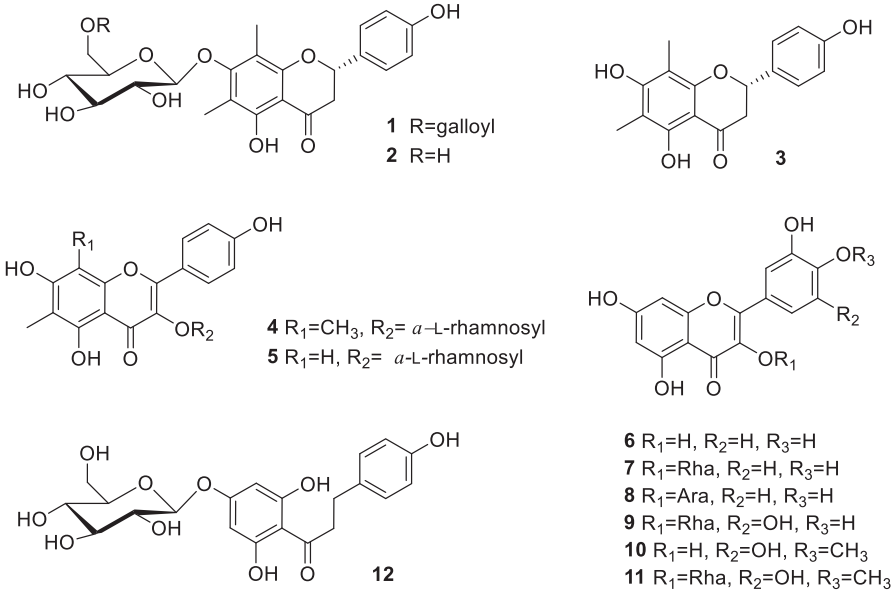

Fig. 1 Structures of compounds **1**–**12**.

silica gel 60 (Qingdao Marine Chemical, China), 75 μm YMC ODS (YMC, Japan), as well as Sephadex LH-20 (GE Healthcare, Sweden). Further, 0.2 mm silica gel plates (HSGF254, Jiangyou Silica Gel Development, Yantai, China) were utilized for TLC analysis. For visualization, spots were sprayed using H_2SO_4 (10%) and then heated.

2.2. Plant materials

In October of 2016, we harvested the *C. conspersipunctatus* leaves from a living tree on campus of Guangdong Academy of Forestry Sciences, which is situated in China's Guangzhou. Professor Xing was responsible for the species authentication. We stored a voucher specimen at the South China Botanical Garden under IBSC-0241906.

2.3. Extractions and isolations

Approximately 10 kg of air-dried *C. conspersipunctatus* leaves was pulverized, and then extracted using 30 L of aqueous EtOH (95%) for 24 h thrice at ambient temperature. Following suspension in water, the resulting crude extract was subjected to sequential extraction with each 2 L of petroleum ether, EtOAc, as well as *n*-BuOH thrice. Next, silica gel CC was performed on 300 g of petroleum ether- and EtOAc-soluble integrated fractions, followed by gradient elution using 100:0–60:40 (v/v) mixtures of $CHCl_3$–MeOH, so that 10 fractions (Frs A − J) were yielded. Further, 90:10–60:40 (v/v) mixtures of petroleum ether–acetone were utilized to separate the Fr. D (96.1 g) via silica gel CC, so that 10 subfractions (Frs D1-D10) were yielded. ODS CC was employed to separate 23.6 g of Fr. D7 using 50–90% (declining polarity) MeOH solution, so that 10 fractions (Frs D7-1-D7-10) were yielded. ODS CC was again employed to separate each 7.1 g of Fr. D7-5 using 40–90% (declining polarity) MeOH solution, so that Frs D7-5-1-D7-5-8 were yielded. This was followed by preparative HPLC purification of each 10-mg sample of Fr. D7-5-7 (2.0 g) using MeOH (60%), thereby yielding 5 mg of compound **3**. ODS CC was performed to separate 34.1 g of Fr. F using 30–90% MeOH solution, so that Frs F1-F8 were yielded. Preparative HPLC was performed on 10-mg sample of Fr. F1 (3.0 g) with MeOH (40%) to derive Compound **9** (5 mg), whereas compound **4** (3 mg) was derived by the same method from 10-mg sample of Fr. F5 (3.2 g) using 50% MeOH. Meanwhile, 90:10–30:10 (v/v) mixtures of petroleum ether–acetone were utilized to separate Fr. G (25.5 g) via silica gel CC, so that 9 subfractions (Frs G1-G9) were yielded, followed by ODS CC separation of 5.4 g of Fr. G4 using 30–90% (declining polarity) MeOH solution, so that 10 fractions (Frs G4-1-G4-10) were yielded. Preparative HPLC purification proceeded on each 10-mg sample of Fr. G4-4 (0.4 g), Fr. G4-6 (2.7 g), Fr. G4-7 (0.24 g), Fr. G6 (0.2 g), Fr. G7 (0.23 g), Fr. G8 (0.26 g), and Fr. G9 (0.09 g) using 60% CH_3CN, 25% MeOH, 23% CH_3CN, 23% CH_3CN, 23% CH_3CN, 22% CH_3CN, and 22% CH_3CN, thereby yielding compounds **2** (3 mg), **12** (3 mg), **5** (3 mg), **10** (3 mg), **6** (3 mg), **11** (3 mg), and **7** (3 mg), respectively. Finally, 90:10–60:40 (v/v) mixtures of $CHCl_3$-MeOH were utilized to separate Fr. H (20.8 g) via silica gel CC, so that 9 subfractions (Frs H-1-H-9) were yielded, followed by the preparative HPLC purification of each 10 mg sample of Fr. H-1 (3.0 g) and Fr. H-3 (0.16 g) with 23% CH_3CN and 10% CH_3CN to afford compounds **1** (3 mg) and **8** (3 mg), respectively.

2.4. ECD calculation

Gaussian 09 package was utilized to compute the ECD of compound **1** in the gas phase at 298.15 K. Adopting the Molecular Merck force field (MMFF) force fields, conformational searching was accomplished at the molecular mechanical level (Li et al., 2013). Screening and subsequent optimization of conformers with lowest energy (relative energy scope: 10 kcal/mol) were accomplished at the level of B3LYP-D3(BJ)/Def2-SVP/PCM(MeOH). TDDFT (time-dependent density functional theory) was employed for computation of ECD spectra based on the screened lowest-energy conformers, which was accomplished at the hybrid PBE0 and M06-2X functionals, as well as the triple zeta valence plus polarization (TZVP; Ahlrichs' basis set) with the solvation model PCM for MeOH.

2.5. α-Glucosidase inhibitory activity assay

Microtiter 96 well microplates were used to conduct the assay by a prior method (Yang et al., 2016; Du et al., 2021). Initially, DMSO was used to dissolve and dilute the compounds to the corresponding concentrations. The positive control is corosolic acid (Zhang et al., 2017a,b) from our previous work (Du et al., 2021). Then, pH 6.8 PBS (67 mM; Thermo Fisher Scientific, Shanghai, China) was used to separately dissolve the α-glucosidase from *Saccharomyces cerevisiae* (10 units/mg, EC 3.2.1.20; Sigma-Aldrich, Shanghai, China) to 0.5 U/mL, as well as the *p*-nitrophenyl α-D-glucopyranoside (*p*-NPG) substrate (J & K Scientific, Beijing, China) to 5 mM. Each assay well included sample (8 μL), PBS (112 μL) and enzyme (20 μL). Each blank well included sample (8 μL) and PBS (132 μL). Each negative control well included DMSO (8 μL), PBS (112 μL) and enzyme (20 μL). Each negative blank well included DMSO (8 μL) and PBS (132 μL). After elaborative shaking to allow complete mixing, the microplates were subjected to a 15 min storage at 37 ℃.Next, each well was incorporated with *p*-NPG (20 μL), mixed well, followed by a further 15 min incubation at 37 ℃. The reaction was then terminated by incorporating 0.2 M sodium carbonate (80 μL) into the buffer. For quantification of α-glucosidase hydrolysate of *p*-nitrophenol from *p*-NPG, the 405 nm OD value of *p*-nitrophenol wass assessed. The assay was triplicated for sample at each concentration. Final step was computation of IC_{50} and relevant presentation as means ± SDs.

2.6. Cytotoxicity assay

All experimental cells, including the human cervix adenocarcinoma (HeLa), non-small cell lung cancer (A549), hepatocellular carcinoma (HepG2) and breast cancer (MCF-7) cell lines, were from the CAS Kunming Institute of Zoology situated in China's Kunming. MTT assay was employed to examine how the compounds were cytotoxic against the foregoing cells by a prior approach (Shi et al., 2014; Wu et al., 2015). Positive control adopted was adriamycin (ADM).

2.7. Molecular docking

Since the X-ray crystallographic structure *S. cerevisiae* α-glucosidase isn't accessible, the source of *S. cerevisiae* α-glucosidase was from AlphaFold Protein Structure Database (https://alphafold.ebi.ac.uk; Jumper et al., 2021; Varadi et al., 2021) under ID: AF-P38158-F1. Molecular docking for the α-glucosidase–compounds interplay were conducted with AutoDock Vina 1.2.0 (https://vina.scripps.edu; Trott and Olson, 2010). At CHARMm force field (http://mackerell.umaryland.edu; Vanommeslaeghe et al., 2010; Klauda and Brooks, 2008; Song et al., 2019), the 3D structure of each molecule energy minimization was accomplished. Before preparation of auto dock format of protein, the water molecules were removed by AutoDockTools 4.2.6 (https://autodock.scripps.edu). The center of the grid box was placed at x = 22.625, y = −8.069 and z = 24.158 (Peytam et al., 2021). The dimensions of the active site box were set at 60 × 60 × 60 Å. Each docked system was carried out by 100 runs of the AutoDock Vina search. The best pose of each ligand was selected for analyzing the interactions between α-glucosidase and the inhibitor. The substrate orientation that gave the lowest interaction energy was chosen for post-docking analysis, and the binding situation that resulted in the lowest docking energy was used for further analyses. The binding conformation was visualised using Discovery studio visualizer 3.0 (https://discover.3ds.com/discovery-studio-visualizer-download).

3. Results and discussion

3.1. The compounds isolated from *C. conspersipunctatus*

The 11 known compounds (Fig. 1) were identified as farrerol 7-*O*-*β*-D-glucopyranoside (**2**) (Quang et al., 2008), (−)-farrerol (**3**) (Youssef et al., 1998), 6, 8-dimethylkaempferol-3-*O*-α-L-rhamnoside (**4**) (Lu et al., 2008), 6-*C*-methylquercetin 3-*O*-α-L-rhamnopyranoside (**5**) (Quang et al., 2008), quercetin (**6**) (Li et al., 2009), quercetin-3-rhamnoside (**7**) (Fossen et al., 1999) quercetin-3-*O*-α-L-arabinopyranoside (**8**) (Kadota et al., 1990), myricitrin (**9**) (Kim et al., 2013), mearnsetin (**10**) (Abbas et al., 2007), mearnsitrin (**11**) (Suedee et al., 2014), and trilobatin (**12**) (Zhang et al., 2017a,b) through relevant spectroscopic investigation combined with comparison with literature data.

Based on HRESIMS, the molecular formula of the novel compound **1** was $C_{30}H_{30}O_{14}$. According to the ^{1}H NMR result in Table 1, two aromatic methyl signals appeared at δ_H 2.01 and 2.10 for the compound **1**, and the resonances of protons at δ_H 7.28 (2H, d, J = 8.8 Hz) and 6.84 (2H, d, J = 8.8 Hz) were characteristic of *p*-substituted phenyl ring. Similarly, three characteristic resonances at δ_H 5.25 (1H, dd, J = 12.8, 3.8 Hz), 3.10 (1H, dd, J = 16.0, 12.8 Hz) and 2.71 (1H, dd, J = 16.0, 3.8 Hz) were ascribed to the C ring of a flavanone moiety. At δ_H 4.73 (1H, d, J = 7.8 Hz), an anomeric proton signal was noticed. The large J values of anomeric proton suggested its configuration was *β*-D-glucose. Analysis of ^{13}C NMR spectra of **1** (Table 1), jointly with the HSQC data, indicated that the structure was tightly associated with farrerol 7-*O*-*β*-D-glucopyranoside (**2**) (Quang et al., 2008). Spectral differences in compound **1** were prominent, while extra two proton signals were present at δ_H 6.95 (2H, d, J = 2.7 Hz), as well as seven carbon signals [δ_C 168.3 (CO), 146.3, 139.6 (2C), 110.1 (2C), 121.4] for a galloyl group. Based on the long-range associations between galloyl carboxyl carbon signals at δ_C 168.3 and two methylene proton signals of glucose H-6″ in the HMBC spectrum, the ester was estimated to localize at glucose C-6″ (Fig. 2). The galloyl group was further confirmed to localize at glucose C-6″, as evidenced by the downfield shift in the glucose C-6″ (δ_C 64.6) and H-6″ [δ_H 4.55 (1H, dd, J = 11.6, 6.3 Hz), δ_H 4.32 (1H, dd, J = 11.7, 2.0 Hz)], moreover the C-5″ was upfield shifted to δ_C 75.6 ppm. Besides, as verified by the HMBC between C-7 (δ_C 162.1) and glucose anomeric proton (δ_H 4.73, d, J = 7.8 Hz), attachment of the 6″-*O*-galloylglucopyranosyl moiety to the eriodictyol 7-hydroxyl group was found. By comparing the TDDFT-based simulated vs. experimental ECD spectra, we inferred the C-2 definite stereochemistry for compound **1**. Preferable consistency was noted between the ECD simulations of compound **1** and the ECD computations of (2*S*)-**1** (Fig. 3). Thus, the compound **1** was structurally recognized as farrerol 7-*O*-*β*-D-(6-*O*-galloyl)glucopyranoside.

3.1.1. Farrerol 7-O-β-D-(6-O-galloyl)glucopyranoside (1)

Yellow powder; $[\alpha]_D^{20}$ + 11.3 (*c* 0.22, CH_3OH); ^{1}H and ^{13}C NMR data were reported in Table 1; ESI(+)MS *m/z* 615.0 $[M + H]^+$; ESI(−)MS *m/z* 613.0 $[M - H]^-$; HRESI(−)MS *m/z* 613.1563 $[M - H]^-$ (calcd for $C_{30}H_{29}O_{14}$, 613.1563).

3.2. The α-glucosidase inhibitory activity and cytotoxicity of compounds 1–3

Assessments were carried out concerning the α-glucosidase-suppressing effects of compounds **1**–**3**. Clearly from Table 2, inhibitory effects were present with the novel compound **1** (IC_{50}: 6.9 ± 1.2 μM) and the established compound **3** (IC_{50}: 21.3 ± 1.1 μM). Compound **1** was found more active than corosolic acid, an established α-glucosidase inhibitor as previously described (Hou et al., 2009; Ni et al., 2019; Zhang et al., 2017a,b; Ouyang et al., 2018) (IC_{50} = 15.5 ± 0.9 μM). As demonstrated by a preliminary exploration of structure–activity relationship (SAR), the inhibitory activity of α-glucosidase disappeared after the glycosidation of flavonoids, and such activity was significantly enhanced by the galloyl group attached to glucose in the flavonoids (**3** vs. **2** vs. **1**). Further cytotoxicity assessment revealed insignificant action of compound **1**–**3** against the tested A549, HeLa, HepG2 and MCF-7 cells, with IC_{50} > 10 μM.

3.3. The molecular docking of compounds 1–3 with α-glucosidase

The potential interaction of compounds **1**–**3** with α-glucosidase were analyzed by molecular docking using previously described methods (Xiong et al., 2018). Corosolic acid and acarbose were used as reference molecules in docking study. The results were shown in Figs. 4-5 and Table 3. Compounds **1**, **2**, **3**, corosolic acid and acarbose could bind to α-glucosidase, whose binding energies were −9.0, −9.2, −8.4, −9.0, −8.2 kcal/mol at lowest, respectively. For compound **1**, its ketone carbonyl group (C-4, galloyl group), hydroxy group (C-3‴) and 6″-O interacted with Lys155 (2.73), Asn314

Table 1 NMR spectroscopic data in Pyridine d_5 [^{1}H at 500 MHz, ^{13}C at 125 MHz] of compound **1.**

position	δ_H mult. (*J* in Hz)	δ_C, type	Position	δ_H mult. (*J* in Hz)	δ_C, type
2	5.25 dd (12.8, 3.8)	80.3, CH	Me-6	2.01 s	9.7, CH_3
3	*β* 2.71 dd (16.0, 3.8) *α* 3.10 dd (16.0, 12.8)	44.6, CH_2	Me-8	2.10 s	9.0, CH_3
4	–	199.9, C	1″	4.73 d (7.8)	105.1, CH
5	–	159.7, C	2″	3.58 t (8.2)	75.6, CH
6	–	111.7, C	3″	3.48 m	78.0, CH
7	–	162.1, C	4″	3.34p (1.6)	72.1, CH
8	–	112.9, C	5″	3.34p (1.6)	75.6, CH
9	–	159.3, C	6″	*β* 4.32 dd (11.7, 2.0) *α* 4.55 dd (11.6, 6.3)	64.6, CH_2
10	–	106.3, C	1‴	–	121.4, C
1′	–	131.5, C	2‴ 6‴	6.95 d (2.7)	110.1, CH
2′ 6′	7.28 d (8.8)	128.9, CH	3‴ 5‴	–	139.6, C
3′ 5′	6.84 d (8.8)	116.3, CH	4‴	–	146.3, C
4′	–	158.8, C	C═O	–	168.3

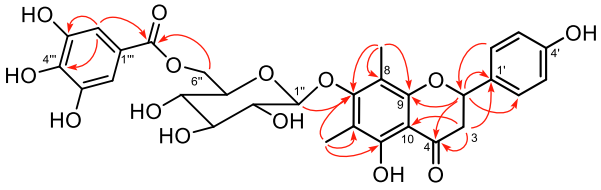

Fig. 2 Key HMBC (plain arrows) correlations of compound **1**.

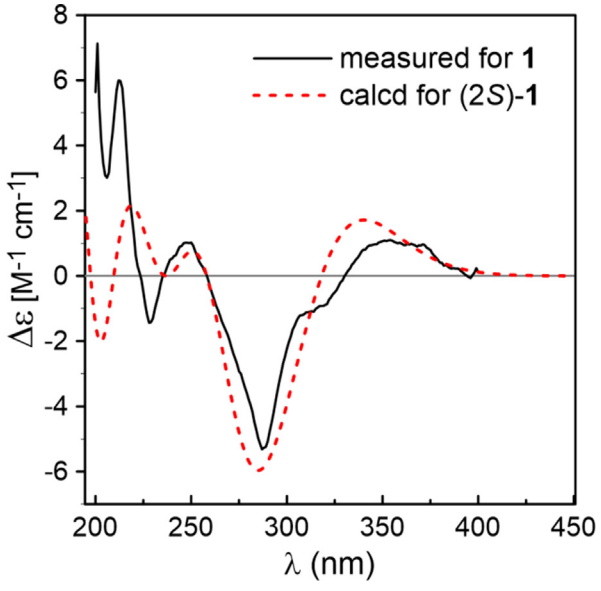

Fig. 3 Comparison of the measured ECD spectrum of compound **1** in MeOH with the PBE0/TZVP/PCM calculated spectrum of (2*S*)-**1**.

(3.19), Ilp315 (2.89), and Lys425 (3.35) residues of α-glucosidase through four hydrogen bonds, respectively. Compound **1** also created π-π interaction with Phe311 (3.77, 4.78), Asp429 (3.59). Whereas the hydroxy groups at C-5, C-6″ of compound **2** form three hydrogen bonds with residues, Phe310 (2.49, 6.34) and Asn314 (2.40) of α-glucosidase. And ketone carbonyl group (C-4) and 7-O interacted with the

Table 2 α-Glucosidase inhibitory activity of compounds **1**–**3** and corosolic acid.

Compound	$IC_{50(\mu M)}$[a]
Farrerol 7-*O*-*β*-D-(6-*O*-galloyl)glucopyranoside (**1**)	6.9 ± 1.2
Farrerol 7-*O*-*β*-D-glucopyranoside (**2**)	NI[b]
(−)-farrerol (**3**)	21.3 ± 1.1
Corosolic acid	15.5 ± 0.9

[a] Values represent means ± SD based on three individual experiments.
[b] NI = NO Inhibition.

Lys155 (4.66), Asn314 (2.27). Moreover, compound **2** formed π-π interaction with Phe311 (4.32), Phe420 (4.72). Compound **3** possessed one hydrogen bonds with residues Lys155 (5.43) with ketone carbonyl group (C-4). In addition, compound **3** formed π-π interaction with Phe311 (4.39), Ile415 (5.12) (Fig. 5). Docking revealed that ketone carbonyl group (C-4) and phenyl ring A were crucial to the inhibitor actions of the flavonoids with Lys155, Phe311, Phe420, respectively. As observed from the best docking conformations, showed that all three compounds have lower free binding energys than acarbose (−8.2 kcal/mol). Therefore, the results emphasized that the target compounds bind more easily to the target enzyme (α-glucosidase) than the reference drug (acarbose). The foregoing findings would contribute to designing and developing α-glucosidase inhibitors with better potencies.

3.4. Biosynthetic pathway of flavonoids isolated from C. conspersipunctatus

The biosynthetic pathway of flavonoids has been generally elucidated from studies in numerous plant species. Thus, enzymes catalyzing flavonoid biosynthesis have been analyzed in various plant species, such as *Gramineous* plants (Jiang et al., 2020), *Vernonia amygdalina* (Shui et al., 2021), *Camellia sinensis* (Liu et al., 2012) and *Myritacea* plants (Koirala et al., 2016). We tried to propose the biosynthetic pathway of isolated compounds and the results were shown in Fig. 6. For the cinnamate-4-hydroxylase (C4H)-catalyzed reaction of *p*-coumaric acid, the branch point is cinnamic acid, which is

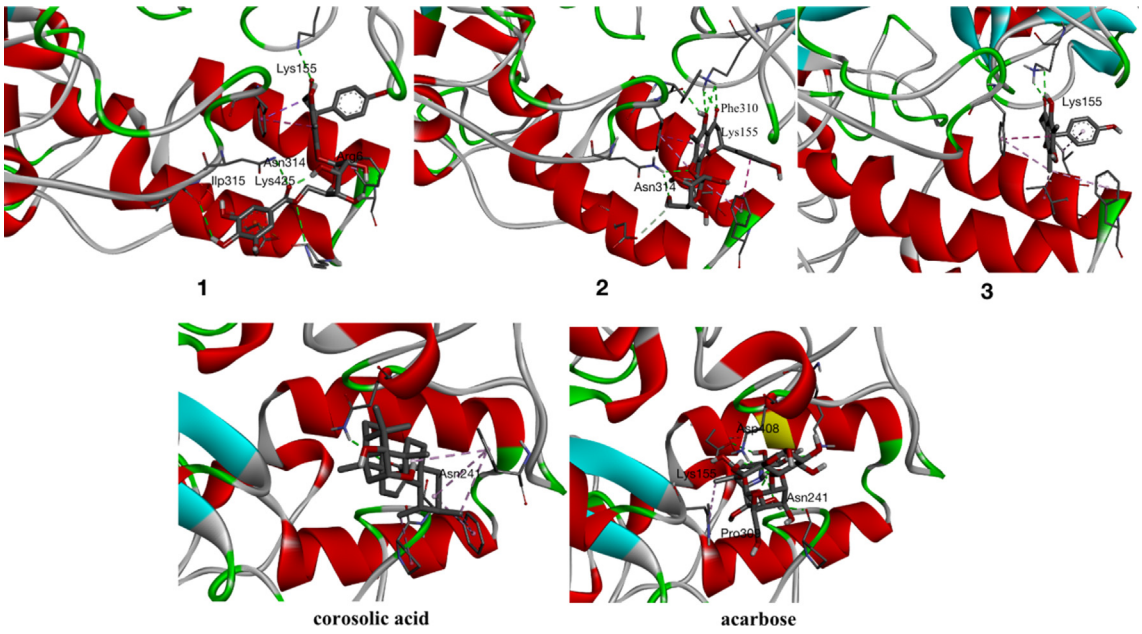

Fig. 4 Compounds **1**–**3**, corosolic acid and acarbose bind with α-glucosidase.

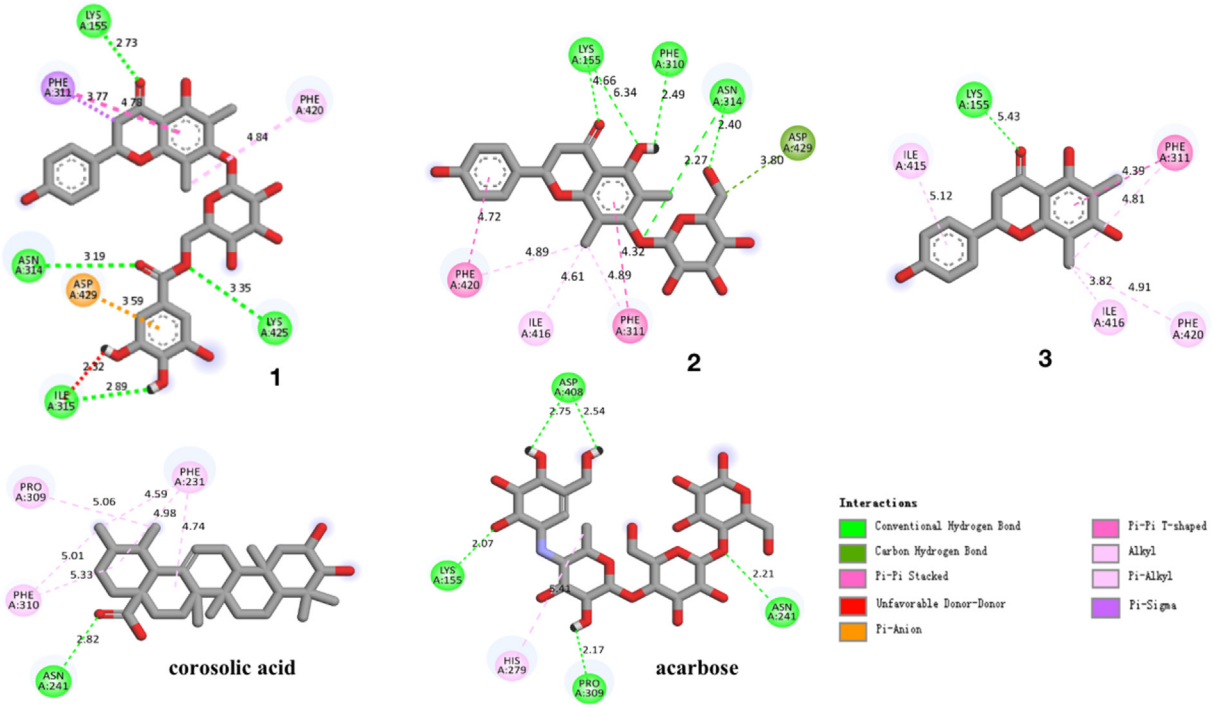

Fig. 5 Interactions of compounds **1**–**3**, corosolic acid and acarbose with α-glucosidase.

generated from the phenylalanine ammonia lyase (PAL)-catalyzed conversion of phenylalanine. *p*-Coumaric acid might be converted to *p*-coumaric-CoA by 4-coumarate CoA ligase (4CL) and further by chalcone synthase (CHS) to naringenin chalcon and then by chalcone isomerase (CHI) and CMT (*C*-methyltransferase) to compound **3**. Compound **3** could be transformed to Compound **2** by F7GlcT (flavonol 7-*O*-glucosyltransferase) and by *O*-galloyltransferase (OGT) to compound **1**. Compound **3** is converted into syzalterin by flavone synthase (FNS). Further hydroxylation by flavanone 3-hydroxylase (F3H) and followed by flavonol 3-*O*-rhamnosyltransferase (F3RhaT) furnishes compound **4**. The naringenin chalcone is transformed into naringenin by CHI or into compound **12** by F7GlcT. By combining the activity of the CMT, F3H and F3RhaT, naringenin might be possible to generate compound **5** or compound **6** by FNS, flavonoid-3′-

Table 3 Interaction information of compounds **1**–**3**, corosolic acid and acarbose with α-glucosidase.

Compounds	Interaction amino acids	Hydrogen bonds	Binding energy (kcal/mol)
1	Lys155, Phe311, Asn314, Ilp315, Phe420, Lys425, Asp429	Lys155, Asn314, Ilp315, Lys425	−9.0
2	Lys155, Phe310, Phe311, Asn314, Ile416, Phe420, Asp429	Lys155, Asn314, Phe310	−9.2
3	Lys155, Phe311, Ile415, Ile416, Phe420	Lys155	−8.4
corosolic acid	Asn241, Phe231, Pro309, Phe310	Asn241	−9.0
acarbose	Lys155, Asn241, His279, Pro309, Asp408	Lys155, Asn241, Pro309, Asp408	−8.2

hydroxylase (F3′H) and F3H. Compound **6** then might be transformed into compound **7**, compound **8** by F3RhaT, flavonol 3-*O*- arabinosyltransferase (F3AraT), respectively. Compound **6** also might be converted to compound **9** by flavonoid 3′,5′-hydroxylase (F3′5′H) and F3RhaT and then generated compound **10** by *O*-methyltransferase (OMT), which finally transformed to compound **11** by F3RhaT.

4. Conclusions

The study on the chemical ingredients and medical-value of *C. conspersipunctatus* afforded one new *C*-methyl flavonoid (**1**) along with 11 known analogues (**2**–**12**). It offers the foundation for further studying of the other plants of the same genus. In this study, the α-glucosidase inhibitory effects of compounds **1**–**3** were assessed with a known inhibitor corosolic acid as positive control. Compound **1** displayed potent α-glucosidase inhibitory effect with an IC_{50} value of 6.9 ± 1.2 μM, being better than corosolic acid (IC_{50}: 15.5 ± 0.9 μM). Compounds **1**–**3** showed negligible effects against A549, HeLa, HepG2 and MCF-7 cells. Meanwhile, molecular docking was employed to explore the probable mechanism for α-glucosidase–compounds **1**–**3** interaction. The results were expected to facilitate the research and development of stronger α-glucosidase inhibitors, where the flavonoid would act as the lead medicinal chemical compound. This work also laid a foundation for pharmacological activity research of the leaves of *C. conspersipunctatus* and provided a theoretical basis for the sustainable utilization of the plant. The result could be also provided a lead compound for the development of novel α-glucosidase inhibitor. Apart from making contribution to comprehending the biosynthetic mechanisms of flavonoids in *C. conspersipunctatus* leaves, our findings also offer valuable data for potential metabolic engineering.

Declaration of Competing Interest

The authors declare that they have no known competing financial interests or personal relationships that could have appeared to influence the work reported in this paper.

Acknowledgements

We thank Mr. Yunfei Yuan, South China Botanical Garden, Chinese Academy of Sciences, for NMR spectroscopic mea-

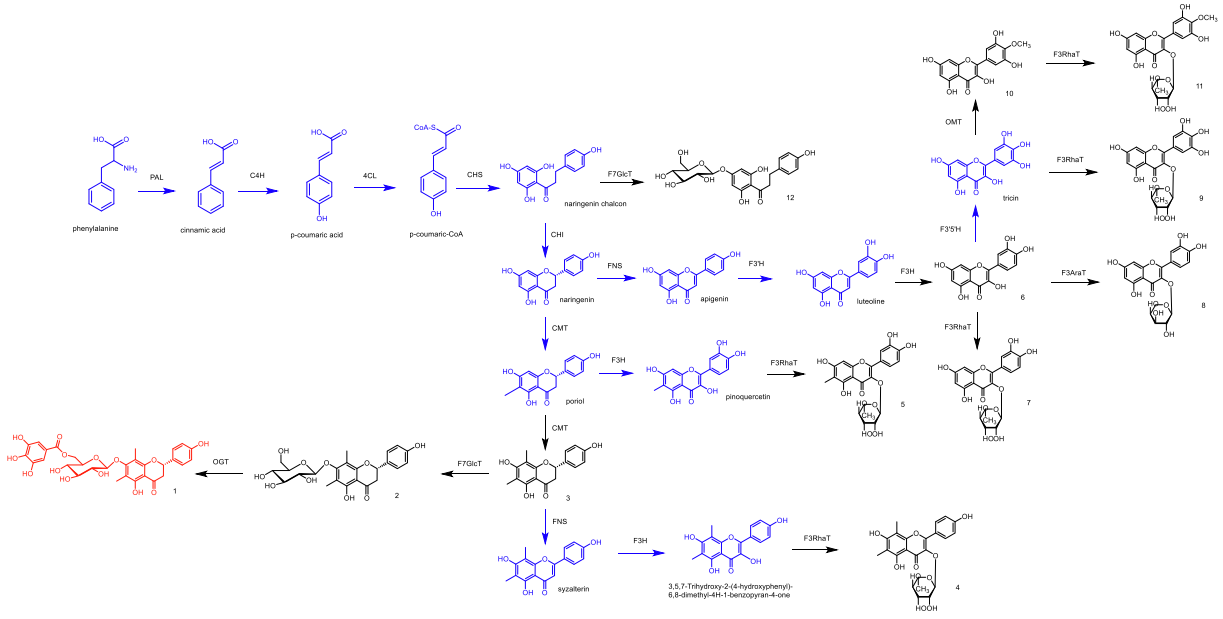

Fig. 6 The proposed biosynthetic pathway of flavonoids isolated from *C. conspersipunctatus* (red: new compound, black: known compounds, blue, inferred compounds). **Enzyme abbreviations:** PAL, phenylalnine ammonia-lyase; C4H, cinnamate-4-hydroxylase; 4CL, *p*- coumaroyl:CoA-ligase; CHS, chalcone synthase; CHI, chalcone isomerase; CMT, *C*-methyltransferase, FNS, flavone synthase; F3H, flavanone 3-hydroxylase; F3′H, flavonoid-3′-hydroxylase; F3′5′H, flavonoid 3′,5′-hydroxylase; OMT, *O*-methyltransferase; F7GlcT, flavonol 7-*O*-glucosyltransferase; F3RhaT, flavonol 3-*O*-rhamnosyltransferase; F3AraT, flavonol 3-*O*- arabinosyltransferase; OGT, *O*-galloyltransferase.

surements, and Ms. Aijun Sun, South China Sea Institute of Oceanology, Chinese Academy of Sciences, for HRESIMS measurements. We gratefully acknowledge support from the Guangzhou Branch of the Supercomputing Center of Chinese Academy of Sciences. This work was supported by the Key-Area Research and Development Program of Guangdong Province (No. 2020B1111110007); the National Natural Science Foundation of China (Nos. 31470423 and 81202398); The special foundation of Guangzhou Key Laboratory (No. 202002010004); Science and Technology Planning Project of Guangdong Province (No. 2017B030314166); Special Funds for State Key Laboratory of Dampness Syndrome of Chinese Medicine (Nos. SZ2021ZZ33, SZ2021ZZ36, SZ2021ZZ40 and SZ2021ZZ46).

Appendix A. Supplementary material

Supplementary data associated with this article including 1D and 2D NMR spectra and HRESIMS of compound **1** are available.

Supplementary data to this article can be found online at https://doi.org/10.1016/j.arabjc.2022.103687.

References

Abbas, F.A., Al-Massarany, S.M., Khan, S., Al-Howiriny, T.A., Abourashed, E.A., 2007. Phytochemical and biological studies on Saudi Commiphora opobalsamum L. Nat. Prod. Res. 21, 383–391.

Chiba, S., 1997. Molecular mechanism in alpha-glucosidase and glucoamylase. Biosci. Biotechnol. Biochem. 61, 1233–1239.

Du, H.F., Li, H.X., Wu, P., Wang, C., Wei, X.Y., 2021. α-glucosidase inhibitory pentacyclic triterpenoids from the leaves of *cleistocalyx conspersipunctatus*. Phytochem. Lett. 41, 109–113.

Editorial Committee of Flora of China, 1984. Flora of China vol. 53, 119.

Editorial Committee of the Administration Bureau of Traditional Chinese Medicine, 1999. Chinese materia medica (Zhong Hua Ben Cao). Shanghai Sci. Technol. Press, Shanghai. 5, 627−629.

Fang, H.L., Liu, M.L., Li, S.Y., Song, W.Q., Hui, O.Y., Zhu, P.X., Zhu, H.L., 2022. Identification, potency evaluation, and mechanism clarification of α-glucosidase inhibitors from tender leaves of *Lithocarpus polystachyus* Rehd. Food Chem. 371, 131128.

Fossen, T., Larsen, S., Kiremire, B.T., Andersen, Y.D.M., 1999. Flavonoids from blue flowers of *Nymphaèa caerulea*. Phytochemistry 51, 1133–1137.

Hou, W., Li, Y., Zhang, Q., Wei, X., Peng, A., Chen, L., Wei, Y., 2009. Triterpene acids isolated from *Lagerstroemia speciosa* leaves as α-glucosidase inhibitors. Phytother. Res. 23, 614–618.

Jiang, B., Song, J., Jin, Y.A., 2020. Flavonoid Monomer Tricin in *Gramineous* Plants: Metabolism, Bio/Chemosynthesis, Biological Properties, and Toxicology. Food Chem. 320, 126617.

Jumper, J., Evans, R., Pritzel, A., et al, 2021. Highly accurate protein structure prediction with AlphaFold. Nature 596, 583–589.

Kadota, S., Takamori, Y., Nyein, K.N., Kikuchi, T., Tanaka, K., Ekimoto, H., 1990. Constituents of the leaves of *Woodfordia fruticosa* Kurz. I. Isolation, structure, and proton and carbon-13 nuclear magnetic resonance signal assignments of woodfruticosin (woodfordin C), an inhibitor of deoxyribonucleic acid topoisomerase II. Chem. & Pharm. Bull. 38, 2687–2697.

Koirala, N., Thuan, N.H., Ghimire, G.P., Thang, D.V., Sohng, J.K., 2016. Methylation of flavonoids: Chemical structures, bioactivities, progress and perspectives for biotechnological production. Enzyme. Microb. Tech. 86, 1–45.

Kim, H.H., Kim, D.H., Kim, M.H., Oh, M.H., Kim, S.R., Park, K.J., Lee, M.W., 2013. Flavonoid constituents in the leaves of *Myrica rubra* sieb. et zucc. with anti-inflammatory activity. Arch. Pharm. Res. 36, 1533–1540.

Klauda, J.B., Brooks, B.R., 2008. CHARMM Force Field parameters for nitroalkanes and nitroarenes. J. Chem. Theory. Comput. 4, 107–115.

Li, J., Jiang, H., Shi, R., 2009. A new acylated quercetin glycoside from the leaves of *Stevia rebaudiana* Bertoni. Nat. Prod. Res. 23, 1378–1383.

Li, Q.M., Ren, J., Zhou, B.D., Bai, B., Liu, X.C., Wen, M.L., Zhu, H. J., 2013. Determining the absolute configuration of benzopyrenomycin by optical rotation, electronic circular dichroism, and population analysis of different conformations via DFT methods and experiments. Tetrahedron 69, 3067–3074.

Liu, G., Yang, N., Wang, X., 2012. Purification and characterization of a novel galloyltransferase involved in catechin galloylation in the tea plant (*Camellia sinensis*). J. Biol. Chem. 53, 44406–44417.

Lu, W.J., Ya, Q.K., Chen, J.Y., Liu, B.M., 2008. A new flavonol glycoside from *Baeckea Frutescens* L. Acta Pharm. Sin. 43, 1032–1035.

Ni, M., Pan, J., Hu, X., Gong, D., Zhang, G., 2019. Inhibitory effect of corosolic acid on α-glucosidase: kinetics, interaction mechanism, and molecular simulation. J. Sci. Food Agric. 99, 5881–5889.

Ning, Z.W., Zhai, L.X., Huang, T., Peng, J., Hu, D., Xiao, H.T., Wen, B., Lin, C.Y., Zhao, L., Bian, Z.X., 2019. Identification of α-glucosidase inhibitors from *cyclocarya paliurus* tea leaves using UF-UPLC-Q/TOF-MS/MS and molecular docking. Food & Funct. 10, 1893.

Ouyang, J.K., Dong, L.M., Xu, Q.L., Wang, J., Liu, S.B., Qian, T.Y., Tan, Y.F., Wen, J., 2018. Triterpenoids with α-glucosidase inhibitory activity and cytotoxic activity from the leaves of *Akebia trifoliata*. Rsc Adv. 8, 40483–40489.

Peytam, F., Takalloobanafshi, G., Saadattalab, T., et al, 2021. Design, synthesis, molecular docking, and in vitro α-glucosidase inhibitory activities of novel 3-amino-2,4-diarylbenzo [4,5] imidazo [1,2-α] pyrimidines against yeast and rat α-glucosidase. Sci. Reports 11, 11911.

Quang, T.H., Cuong, N.X., Minh, C.V., Kiem, P.V., 2008. New flavonoids from *Baeckea frutescens* and their antioxidant activity. Nat. Prod. Commun. 3, 755–758.

Shi, J.F., Wu, P., Jiang, Z.H., Wei, X.Y., 2014. Synthesis and tumor cell growth inhibitory activity of biotinylated annonaceous acetogenins. Eur. J. Med. Chem. 71, 219–228.

Shui, L., Huo, K., Chen, Y., Zhang, Z.L., Niu, J., 2021. Integrated metabolome and transcriptome revealed the flavonoid biosynthetic pathway in developing *Vernonia amygdalina* leaves. PeerJ. 9, e11239.

Song, S.S., Sun, C.P., Zhou, J.J., Chu, L., 2019. Flavonoids as human carboxylesterase 2 inhibitors: Inhibition potentials and molecular docking simulations. Int. J. Biol. Macromol. 131, 201–208.

Suedee, A., Tewtrakul, S., Panichayupakaranant, P., 2014. Anti-HIV-1 integrase activity of *Mimusops elengi* leaf extracts. Pharm. Biol. 52, 58–61.

Trott, O., Olson, A.J., 2010. AutoDock Vina: improving the speed and accuracy of docking with a new scoring function, efficient optimization and multithreading. J. Comput. Chem. 31, 455–461.

Varadi, M., Anyango1 S., Deshpandeet M. et al., 2021. AlphaFold Protein Structure Database: massively expanding the structural coverage of protein-sequence space with high-accuracy models. Nucleic Acids Res. 2021, 1-6.

Vanommeslaeghe, K., Hatcher, E., Acharya, C., Kundu, S., Zhong, S., Shim, J.E., Darian, E., Guvench, O., Lopes, P., Vorobyov, I., MacKerell Jr., A.D., 2010. CHARMM General Force Field (CGenFF): A force field for drug-like molecules compatible with the CHARMM all-atom additive biological force fields. J. Comput. Chem. 31, 671–690.

Wu, P., Yao, L., Xu, L., Xue, J., Wei, X., 2015. Bisacremines A-D, Dimeric acremines produced by a soil-derived *Acremonium persicinum* Strain. J. Nat. Prod. 78, 2161–2166.

Xiong, S.L., Yue, L.M., Lim, G.T., Yang, J.M., Lee, J.h., Park, Y.D., 2018. Inhibitory effect of raspberry ketone on α-glucosidase: Docking simulation integrating inhibition kinetics. Int. J. Biol. Macromol. 113, 212-218.

Yang, D., Xie, H., Jiang, Y., Wei, X., 2016. Phenolics from strawberry cv. Falandi and their antioxidant and α-glucosidase inhibitory activities. Food Chem. 194, 857–863.

Ye, C.L., Lai, Y.F., 2016. 2',4'-dihydroxy-6'-methoxy-3',5'-dimethylchalcone, from buds of *Cleistocalyx operculatus*, induces apoptosis in human hepatoma SMMC-7721 cells through a reactive oxygen species-dependent mechanism. Cytotechnology 68, 331–341.

Youssef, D., Ramadan, M.A., Khalifa, A.A., 1998. Acetophenones, a chalcone, a chromone and flavonoids from *Pancratium maritimum*. Phytochemistry 49, 2579–2583.

Zhang, B.Y., Cao, F., He, P., Yang, X.L., Zhu, H.J., 2017a. Chemical constituents of the fruit of *Schisandra sphenanthera*. Chem. Nat. Comp. 53, 1154–1156.

Zhang, B.W., Xing, Y., Wen, C., Yu, X.X., Dong, Y.S., 2017b. Pentacyclic triterpenes as α-glucosidase and α-amylase inhibitors: Structure-activity relationships and the synergism with acarbose. Bioorg. Med. Chem. Lett. 27, 5065–5070.

Zhu, X.F., Xie, B.F., Zhou, J.M., Feng, G.K., Liu, Z.C., Wei, X.Y., Zhang, F.X., Liu, M.F., Zeng, Y.X., 2005. Blockade of vascular endothelial growth factor receptor signal pathway and antitumor activity of ON-III (2′,4′-Dihydroxy-6′-methoxy-3′,5′-dimethylchalcone), a component from Chinese Herbal Medicine. Mol. Pharmaco. 67, 1444–1450.